Chalcogenide Letters Vol. 19, No. 3, March 2022, p. 173 - 182

Analytical study of gradual photovoltaic $CuInGaSe_2$ based solar cell performances

B. Merah, A. Hemmani*, H. Khachab
Laboratory for the Development of Renewable Energies and their Applications in Saharan Areas (LDERAS), Faculty of Exact Sciences, University TAHRI Mohammed Béchar
Department of Material Sciences, Faculty of Exact Sciences, University TAHRI Mohammed Béchar

The most significant challenge for environment and renewable energy researchers is to achieve good performance, as well as cost efficiency in terms of solar generators especially in the PV sector. Regarding the thin film solar cells based on $Cu(In,Ga)Se_2$, the present work dissertation is concerned with the performance of a graded band gap solar cell based on (CIGS). The aim is to determine the influence of physical and geometrical parameters on performance. Results indicate that the increase in electric field resulting from the gradient of the band gap dismantles the effects of surface recombination. The results obtained are an efficiency of 26 % for Eg_0=1.67 eV, Eg_1=1.02 eV and a thickness of layer p and n d_1=1µm, d_2=2µm respectively.

(Received December 1, 2021; Accepted March 3, 2022)

Keywords: Solar cells, Graded band gap, Performance, (CIGS)

1. Introduction

Recently a considerable effort has been directed toward obtaining efficient solar cells. In particular, CIGS would appear to be the most promising material for solar energy conversion. However, CIGS has a large surface recombination velocity (S= 10^7cm/sec?), which suggests that it will be difficult to obtain large collection efficiencies in this material because electron-hole pairs are created in an extremely thin layer adjacent to the surface and excited by light with a photon energy higher than the band gap at the surface. Accordingly, CIGS cells have hitherto failed to realize their predicted performance and a reduction of the effect of surface recombination is needed to improve the cell performance. The methods of reducing the effect of the surface recombination are of two types: (i) a "window effect" of hetero junctions and (ii) a drift field in the surface layer [2,3,7].

The effect of drift fields is based on impurity distribution gradients, the preparation of semiconducting materials with graded band gaps is very difficult, and to the best of our knowledge, no previous attempt to achieve such structures has been made. CIGS is therefore a material whose Eg can be adjusted between 1.02eV and 1.69eV depending on the gallium content. The optimal value of Eg depends on several factors. From the point of view of photon absorption, it is preferable to have a reduced Eg value, allowing absorbing a larger spectrum (longer wavelengths). This results in a higher current delivered by the solar cell (Jcc). However, it is the value of Eg that determines the maximum voltage delivered by the cell. In order to maximize the conversion efficiency, it is, therefore, necessary to obtain an ideal compromise between current and voltage. Most of the experimental results published in the field of CIGS cells show that the best efficiencies are obtained with a gap of about 1.2eV [8], which corresponds to a Ga rate close to 30%. The presence of a Ga concentration gradient in the absorber layer allows obtaining a variation of the band gap in the thickness of the material. This gap gradient has been the subject of many studies in the field of CIGS.

* Corresponding author: hemmani.abderrahmane@univ-bechar.dz
https://doi.org/10.15251/CL.2022.193.173

In this context, our study emphasizes on the simulation of the gradual photovoltaic CIGS cells performances in standard running conditions to assess the efficiency of photovoltaic conversion.

2. The gradual CIGS based cell structure

2.1. Cell Structure

Adapting a structure is essentially composed of a cell (p- n) based on CIGS, in which is deposited a gradual band gap layer p(Cu $In_{(1-x)}$ Ga_x Se_2), of type P on the illuminated surface N (Cu $InSe_2$).This layer has been inserted to create an electric field, that allows to lower the effective value of the recombination velocity at the surface and consequently to improve the electrical characteristics of the cell. A diagram of the structure is shown in Figure 1.

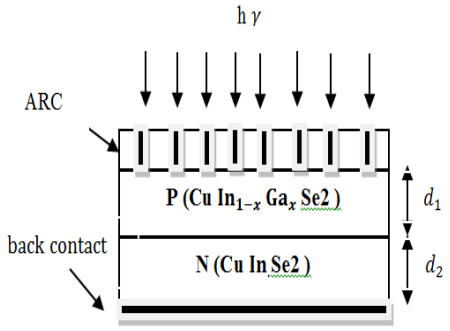

Fig. 1. Schematic representation of the solar cell p($CuIn_{1-x}Ga_xse2$)/ N(CuInSe2).

2.2. Diagram of the Bands

The band gap width of CIGS varies as a function of x between pure CIS and pure CGS values, according to the following empirical law [5]:

$$Eg = 1.010 + 0.626\,x - 0.167\,x\,(1 - x) \quad (1)$$

The cell P (Cu $In_{(1-x)}$ Ga_xSe_2)/N(Cu $InSe_2$). The gradual state of the band gap of the P layer results in an internal field.

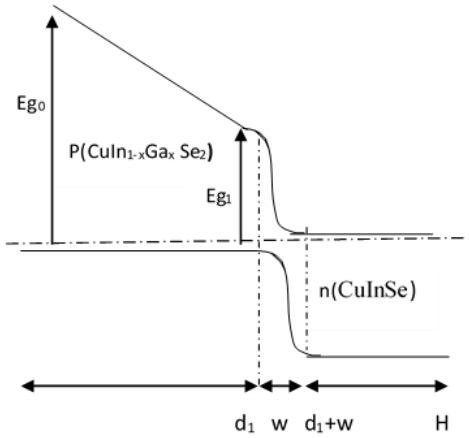

Fig. 2. Diagram of the energies bands of gradual gap solar cell p($CuIn_{1-x}Ga_xse_2$)/ N($CuInSe_2$).

3. Photocurrent Calculation

To determine the current density in a cell, it is necessary to solve the continuity equation in the two regions, namely region p($CuIn_{1-x}Ga_xSe_2$) and region N($CuInSe_2$) and the contribution of the charge zone of the space.

The total photocurrent is the sum of the three photocurrents contributions.

$$J_{ph}(\lambda) = J_n(\lambda) + J_p(\lambda) + J_{ZCE}(\lambda) \tag{2}$$

3.1. Photocurrent density in the region of the transmitter P

The photocurrent is essentially due to the current of the minority electrons. The current density in the transmitter region, characterized by its gradual gap, is given according to the energetic domain.

The continuity equation in the p($CuIn_{1-x}Ga_xSe_2$) layer is determined from the variation of the minority carriers which are, in this case, the photons. It can be written as [1,2]

$$D_n \frac{d^2n}{dx^2} + \mu_n E_i \frac{dn}{dx} - \frac{n}{\tau_n} + g_1(\lambda, x) = 0 \tag{3}$$

$g_1(\lambda, x)$: Expression depends on the considered frequency [2].

3.1.1. Generation Rate

Due to the light absorption in a semiconductor, the photon density N as a function of position within it, according to the Beer's law, is as follows:

$$\partial N / \partial x = -\alpha N \tag{4}$$

where α is the absorption coefficient and x is the position measured from the semiconductor surface. The absorbed photons provide carriers generated at a rate proportional to the photon absorption rate:

$$g_1(\lambda, x) = -\partial N / \partial x = \alpha N \tag{5}$$

We shall consider semiconductors with a linear variation of the band-gap from Eg_0 to Eg_1 as shown in Fig. 2. Then

$$E_i = \frac{E_{g1} - E_{g0}}{d_1} \tag{6}$$

Eg1 is the band-gap at the end of the semiconductor layer having a thickness d1. In this case, the absorption coefficient becomes:

$$\alpha(\lambda, x) = A(h\nu - E_{g1} - E_i x)^{1/2} \tag{7}$$

Solving Eq. (1) with α given by (7), and then substituting into Eq. (5), the electron–hole pair generation rate is

$$g_1(\lambda, x) = -\frac{dN}{dx} = N_0 A\left(h\nu - E_{g1} - E_i x\right)^{1/2} exp\left\{\frac{2A}{3E_i}\left[(h\nu - E_{g0} - E_i x)^{3/2} - \left(h\nu - E_{g0}\right)^{3/2}\right]\right\} \quad h\nu > E_{g0} \tag{8}$$

$$g_1(\lambda, x) = -\frac{dN}{dx} = N_0 A\left(h\nu - E_{g1} - E_i x\right)^{1/2} exp\left\{\frac{2A}{3E_i}\left[(h\nu - E_{g0} - E_i x)^{3/2}\right]\right\} \quad E_{g1} < h\nu < E_{g0} \tag{9}$$

$$X_1 = -\frac{q}{2KT}E_i + \left[\left(\frac{q}{2KT}E\right)^2 + \frac{L}{L_n^2}\right]^{1/2} \tag{10}$$

$$X_2 = -\frac{q}{2KT}E_i - \left[\left(\frac{q}{2KT}E\right)^2 + \frac{L}{L_n^2}\right]^{1/2} \quad (11)$$

$$n(x) = C_1 e^{X_1 x} + C_2 e^{X_2 x} + \frac{1}{X_1 - X_2}[Q_1(x)e^{X_1 x} + Q_2(x)e^{X_2 x}] \quad (12)$$

With α_n and f_n are constants

$$\alpha_n = \frac{\mu_n E_i}{2D_n} \qquad f_n = [\,(\frac{\mu_n E_i}{2D_n})^2 + \frac{1}{L_n^2}\,] \quad (13)$$

where:

$L_{n=(}D_n\tau_n)^{1/2}$: The length of electrons diffusion.

$$Q_1(x) = -\frac{1}{D_n}\int_0^x e^{-X_1 x} g_2(x,\lambda)dx \quad (14)$$

$$Q_2(x) = \frac{1}{D_n}\int_0^x e^{-X_1 x} g_2(x,\lambda)dx \quad (15)$$

The two integration constants C_1 and C_2 of n(x) can be determined from the limit conditions [2].

For x = 0, the minority carriers recombine at the surface at a velocity of recombination Sn,

$$D_n \frac{\partial n}{\partial x}|_0 + \mu_n E_i n(0) = S_n n(0) \quad (16)$$

For: x=d_1, at the junction P-N, in the absence of applied potential difference that is to say, in the condition of short-circuit, the excessive concentrations of minority carriers tend to zero on the junction side.

$$n(d_1) = 0 \quad (17)$$

The photocurrent in the gradual region [2]:

$$J_n(\lambda) = qD_n \frac{dn}{dx} \quad (18)$$

Hence, the photocurrent density in this region will be:

$$J_n(\lambda) = q.\frac{\exp(\alpha_n d_1)}{2}.\frac{\left(\alpha_n - f_n + {}^{S_n}/_{D_n}\right).Q_1(d_1) + \left(\alpha_n - f_n + {}^{S_n}/_{D_n}\right)Q_2(d_1)}{f_n \cosh(f_n d_1) + \left(\alpha_n + {}^{S_n}/_{D_n}\right)\sinh(f_n d_1)} \quad (19)$$

3.2. Contribution of charge zone of space

The current density depends on the absorbed number of photons only per second [7-10], therefore:

$$J_{ZCE}(\lambda) = qN_1(\lambda)[1 - \exp(-\alpha(\lambda)w] \quad (20)$$

With ;

$$N_1 = N_0 \exp(-\alpha d_1)$$

N_1: The flux incident at the charge zone of the space.

W: Width of charge zone of the space.

3.3. Photocurrent density in the region N.

The minorities are the holes for the N type semiconductor. The continuity equation in this region is written as follows [2,3]:

$$D_p \frac{d^2 p}{dx^2} - \frac{p}{\tau_p} + g_2(x) = 0 \quad (21)$$

where: $g_2(x) = \alpha_1(\lambda)N_2 \exp(-\alpha_1(\lambda)x)$ determines the generation rate in the region N.

The solution of this equation is given by

$$\Delta p = A_1 ch\left(\frac{x}{L_p}\right) + B_1 sh\left(\frac{x}{L_p}\right) - \frac{\alpha_1 F(1-R)\tau_p}{\alpha_1^2 L_p^2 - 1}\exp(-\alpha_1 x) \quad (22)$$

where:

$L_P = \sqrt{D_P \tau_p}$: The diffusion length of holes.

The two constants A_1 and B_1 can be found from the conditions at the limits.

At the junction limit, the excess carrier density, reduced to zero by the electrical field in the depletion zone, is interpreted by:

$$\Delta P(x = d_1 + w) = 0 \quad (23)$$

At the surface, a recombination happens with a velocity Sp. The condition is:

$$D_P \frac{dP}{dx} = S_P P \qquad \text{for} \quad x=d_2 \quad (24)$$

The current density in this region is then:

$$J_P(\lambda) = qD_P\left(\frac{dp}{dx}\right)_{d_1+w} \quad (25)$$

$$J_P(\lambda) = \left(q\frac{N_0\alpha_2 L_p}{\alpha_2^2 L_p^2 - 1}\right)\exp[-\alpha_1(d_1 + w_1) - \alpha_2 w_2]\left[\alpha_2 L_p - \frac{\frac{S_p L_p}{D_p} + \left(ch\left(\frac{d_2}{L_P}\right) - \exp(-\alpha_2 d_2)\right) + sh\left(\frac{d_2}{L_p}\right)\alpha_2 L_p \exp(-\alpha_2 d_2)}{\frac{S_p}{D_p} sh\left(\frac{d_2}{L_p}\right) + ch\left(\frac{d_2}{L_p}\right)}\right]. \quad (26)$$

4. Results and discussions

In this part, the simulation results of $P(CuIn_{1-x}Ga_xSe_2)$ / $N(CuInSe_2)$ gradual gap solar cell are exposed, based fundamentally on the modeling of cell electrical behavior. In our approach, we suggest two solar cell structures: Homo-junction solar cell (E = 0 V/cm) and Gradual transmitter solar cells.

The simulation parameters are illustrated in Table1. Describing the physical parameters of different layers of proposed CGIS solar cell:

Table 1. Parameters of the standard cell CdS/CZTS [4, 5, 10,11].

Parameter	**CGS/CIGS**
Thickness, W (nm)	2500
Band gap, Eg (eV)	1.69-1.16
Electron affinity, χ(eV)	4.5
Dielectric permittivity, ε_r	13.6
Effective Density of states, $N_C(cm^{-3})$	2.2×10^{18}
Effective Density of states,$N_V(cm^{-3})$	1.8×10^{19}
Electron mobility, μe (cm^2/Vs)	100
Hole mobility, μp (cm^2/Vs)	25
Donor Concentration, n (cm^3)	1.0×10^{17}
Acceptor Concentration, p (cm^3)	1.0×10^{17}
Surface recombination velocity of electrons (cm/s)	10^7
Surface recombination velocity of holes (cm/s)	10^7
Electron capture cross section $\sigma_n(cm^2)$	10^{-13}

Hole capture cross section σ_p (cm2)	10^{-15}
Densité de défauts, $N_t(cm^{-3})$	10^{14}

For the external parameters used, we take standard conditions, which are:

- The AM1.5 solar spectrum.
- The illumination is 1000W / m².
- The temperature is 300 K.

4.1. The spectral response

4.1.1. Homo-junction CIGS based solar cell

Figure3 represents the spectral response in terms of the wavelength for homo-junction solar cell.

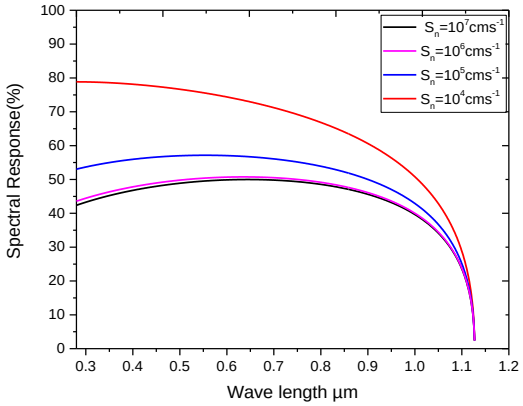

Fig. 3. spectral response of the homojunction solar cell as a function of wavelength for different values of the recombination S_n.

Figure3: Shows that the superficial recombination velocity values Sn = (10^6 and 10^7 cm/s) provoke a remarkable variation of spectral response for all absorbed spectrums $E_{g_1} \leq h\gamma \leq E_{g0}$. By contrast, this effect is weak for the values Sn = [0…10^5] cm/s.

4.1.2. Gradual CIGS based solar cell

Figure 4 illustrates the spectral response in terms of wavelength for the second cell (gradual energy gap cell) for an electric field of 6500V/cm.

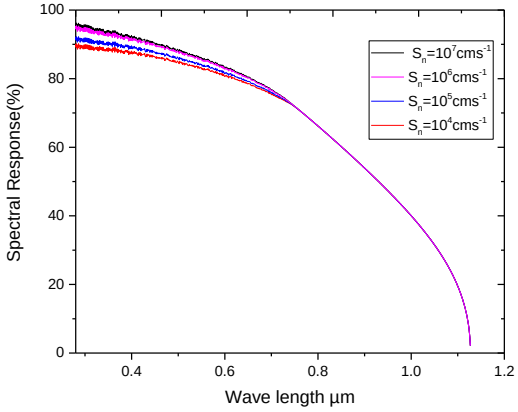

Fig. 4. Spectral response of the gradual gap solar cell in terms of wavelength for different recombination values.

Analysis of figure 4 shows that:

The confrontation of the spectral response curves for values enter [10^4 and 10^5] cm^2/s in the case of the graded cell:

The existence of a variation of the spectral response in the region or ($h\gamma \geq Eg_0$)

Decrease of the spectral response in the region of spectrum ($h\gamma \leq Eg_0$)) what allows us to neglect the effect of surface recombination for velocity value lower than 105 cm2/s; for this reason, we can deduce that the layer p(Cu In $_{(1-x)}$ Ga_x Se_2) plays two roles, one of a window layer and one of an absorbing layer.

4.1.3. Spectral Response in the three regions

Figure5 illustrates of the contribution of the three regions in the spectral response in terms of wavelength for the gradual solar cell P ($CuIn_{1-x}Ga_x$ Se_2)/N ($CuIn.Se_2$). d_1=1µm , d_2=2µm, E_i =6500V/cm.

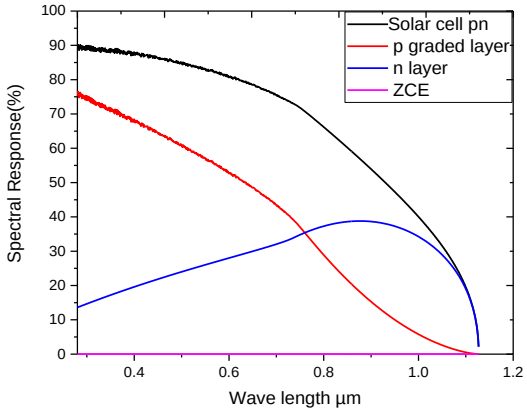

Fig. 5. Spectral response for the three regions.

From Figure 5, one can notice that:

The majority of incident flux is absorbed in the gradual p($CuIn_{1-x}Ga_xSe_2$) layer; this is justified by the number of absorbed photons. The spectral response in the ZCE zone is negligible.

4.2. The photocurrent

The recombination velocity influence on the total current density supplied by the two cells (homo-junction and gradual) is represented in Figure 6.

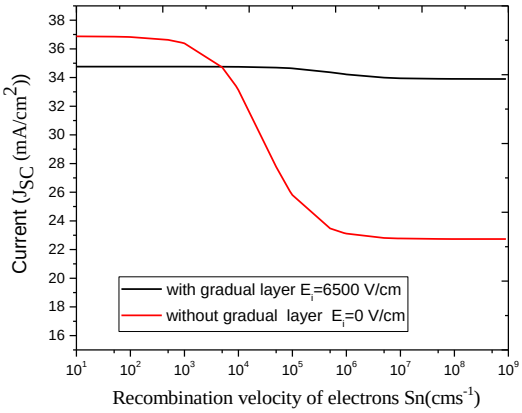

Fig. 6. Recombination velocity influence on the total photocurrent for the two cells (Homo-junction and gradual).

From Figure 6, it is noted that:

The curves show a diminution of current density in comparison with the variation of the recombination velocity value. This decrease is remarkable and rapid in the case of homo-junction cell.

For the first curve that corresponds to the (E_i= 6500V/cm) gradual cell, the current density varies from 36.9mA/cm^2 to 34 mA/cm^2 for a recombination velocity variation of 10^4 to 10^7 cm^2/s. However, this variation is from 34 mA/cm^2 to 22.3 mA/cm^2 in the same recombination velocity interval.

4.2.2. The effect of electric field

Figure7 represents the photocurrent variation in terms of electrical field resulting from the gradient of energy gap for a recombination velocity of Sn = 10^7 cm^2/s.

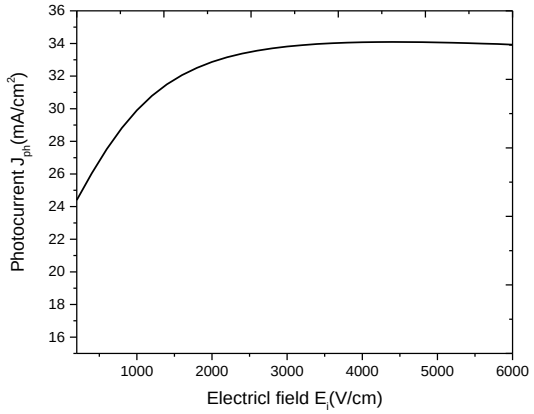

Fig. 7. Photocurrent variation in terms of electrical field for Sn = 10^7 cm^2/s.

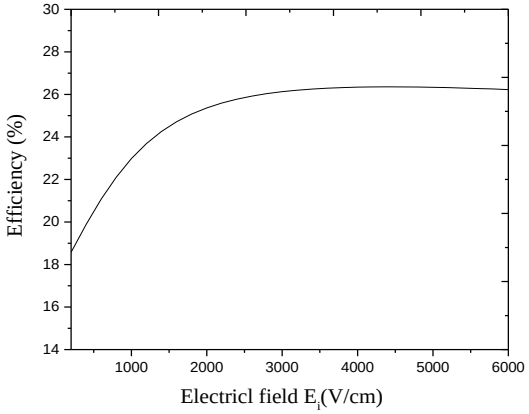

Fig. 8. Efficiency variation in terms of electrical field for Sn = 10^7 cm^2/s.

From figure7, it is noted that:

- The electrical field provokes an increase in the current density value.
- When the electric field varies from 0 to 6500 V/cm, energy gap Eg_0 increases from 1.02 to 1.69 eV.
- The electrical field has a remarkable effect on the photovoltaic conversion efficiency, and this is due to the direct relationship between photocurrent and efficiency as shown in Figure 8.

5. Characteristics J(V)

Here the comparison result of J-V curve is discussed. J-V is one of the most important characteristics of a solar cell, using this feature; we can find open circuit voltage, short circuit current density, fill factor, maximum voltage and maximum current associated with the maximum power. The J-V characteristics of gradual band gap solar cell and homo junction solar cell are shown in Figure 3. In the figure, we can see that the current density of gradual band gap solar cell is higher than the two homo-junction cells.

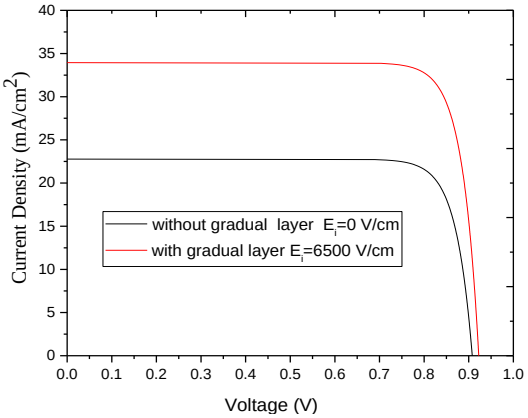

Fig. 9. J-V characteristics comparison curve between homo-junction and gradual band gap solar cell.

Table 2. Illustrates the electrical characteristics of the two cells examined (homo-junction and gradual gap) solar cell.

Performance	Short circuit current (J_{cc} (mA/cm^2))	Open circuit voltage (Vco (V))	Efficiency (**η** (%))	Form Factor) (FF (%))
Homo-junction	22.77	0.907	17.28	83.5
gradual band gap	33.9	0.922	26	83.78

Analysis of the results presented in the previous table shows that the short circuit current density increases from 22.7 mA/cm^2 for a standard CGIS based cell to 33.9 mA/cm^2 for a cell gradual. The graded layer shows an improvement in photovoltaic conversion efficiency from 17.28% to 26%. The open circuit voltage and form factor show a slight increase.

6. Conclusion

In order to minimize the effect of surface recombination losses and to improve the performance of the solar cell, we studied the graded band gap layer in a CIGS-based thin film solar cell.

The deposition of a graded layer shows a significant improvement on the different electrical parameters of the CIGS-based solar cell.

The additional graded band gap layer of the solar cell has a remarkable impact on the electrical characteristics and performance of the solar cell. There is an improvement of the short circuit current and open circuit voltage values as well as the conversion efficiency with acceptable magnitudes.

For example, the photocurrent shows a development from 22 to 34 mA/cm^2. Additionally, photovoltaic conversion efficiency increases from 18 % for a standard solar cell to 26 % for one with a graded band gap layer.

References

[1] M. Trovianon, K. Taretto, Solar Energy Materials & Solar Cells 95, 821 (2011); https://doi.org/10.1016/j.solmat.2010.10.028

[2] M. Konagai.Takahashi, Solid Electronics 19, 259 (1976); https://doi.org/10.1016/0038-1101(76)90172-6

[3] Arturo Morales-Acevedo, Energy Procedia 2, 169 (2010).

[4] S. Amiri, S. Dehghani, R. Safaiee, Optical and Quantum Electronics 52, 323 (2020); https://doi.org/10.1007/s11082-020-02441-2

[5] S. Ouedraogo, R. Sam, F. Ouedraogo, M. B. Kebre, J. M. Ndjaka, F. Zougmore, Journal of Ovonic Research 9(4), 95 (2013).

[6] M. Elbar, S. Tobbeche, Energy Procedia 74, 1220 (2015). https://doi.org/10.1016/j.egypro.2015.07.766

[7] N. Khoshsirat, N. Amziah, Md. Yunus, M. N. Hamidon, S. Shafie, N. Amin, Pertanika J. Sci.& Technol. 23(2), 241 (2015).

[8] B. Barman, P. K. Kalita, Solar Energy 216, 329 (2021); https://doi.org/10.1016/j.solener.2021.01.032

[9] Rasika N. Mohottige, Sandanuwan P. Kalawila Vithanage, Journal of Photochemistry & Photobiology, A: Chemistry 407, 113079 (2021); https://doi.org/10.1016/j.jphotochem.2020.113079

[10] N. El I Boukortt, S. Patan, Optik - International Journal for Light and Electron Optics 218, 165240 (2020); https://doi.org/10.1016/j.ijleo.2020.165240

[11] A. K. Patel, P. K. Rao, R. Mishra, S. K. Soni, Optik - International Journal for Light and Electron Optics 243, 167498 (2021); https://doi.org/10.1016/j.ijleo.2021.167498